

Analytical Methods

Accepted Manuscript



This is an *Accepted Manuscript*, which has been through the Royal Society of Chemistry peer review process and has been accepted for publication.

Accepted Manuscripts are published online shortly after acceptance, before technical editing, formatting and proof reading. Using this free service, authors can make their results available to the community, in citable form, before we publish the edited article. We will replace this *Accepted Manuscript* with the edited and formatted *Advance Article* as soon as it is available.

You can find more information about *Accepted Manuscripts* in the [Information for Authors](#).

Please note that technical editing may introduce minor changes to the text and/or graphics, which may alter content. The journal's standard [Terms & Conditions](#) and the [Ethical guidelines](#) still apply. In no event shall the Royal Society of Chemistry be held responsible for any errors or omissions in this *Accepted Manuscript* or any consequences arising from the use of any information it contains.

1
2
3
4
5
6
7
8
9
10
11
12
13
14
15
16
17
18
19
20
21
22
23
24
25
26
27
28
29
30
31
32
33
34
35
36
37
38
39
40
41
42
43
44
45
46
47
48
49
50
51
52
53
54
55
56
57
58
59
60

Sensitive Detection of Cardiac Biomarkers Using a Magnetic Microbead Immunoassay

Christine F. Woolley
Mark A. Hayes

Department of Chemistry and Biochemistry
Arizona State University
Tempe, AZ, USA

Corresponding author
Dr. Mark A. Hayes
Arizona State University
Department of Chemistry and Biochemistry
Tempe, Arizona 85287-1604
mhayes@asu.edu
480-965-2747 (fax)

Abbreviations:

AMI (acute myocardial infarction), cTnI (cardiac troponin I), H-FABP (heart-type fatty acid binding protein), Pab (polyclonal antibody), μ TAS (micro-total analysis system)

Keywords:

Cardiac biomarker, micro-immunoassay, sandwich immunoassay, microbead immunoassay, assay optimization, quantitation limit

Total Words: 4929

Abstract

To achieve improved sensitivity in cardiac biomarker detection, a batch incubation magnetic microbead immunoassay was developed and tested on three separate human protein targets: myoglobin, heart-type fatty acid binding protein, and cardiac troponin I. A sandwich immunoassay was performed in a simple micro-centrifuge tube allowing full dispersal of the solid capture surface during incubations. Following magnetic bead capture and wash steps, samples were analyzed in the presence of a manipulated magnetic field utilizing a modified microscope slide and fluorescent inverted microscope to collect video data files. Analysis of the video data allowed for the quantitation of myoglobin, heart-type fatty acid binding protein and cardiac troponin I to levels of 360 aM, 67 fM, and 42 fM, respectively. Compared to the previous detection limit of 50 pM for myoglobin, this offers a five-fold improvement in sensitivity. This improvement in sensitivity and incorporation of additional markers, along with the small sample volumes required, suggest the potential of this platform for incorporation as a detection method in a total sample analysis device enabling multiplexed detection for the analysis of clinical samples.

Introduction

Due to their high sensitivity, biosensors have become a popular diagnostic tool for both early and rapid disease detection. Early detection is particularly important in cases of acute myocardial infarction (AMI) where prompt diagnosis is crucial for patient survival. The biomarker targeted by the biosensor is of key importance and the characteristics an ideal cardiac marker have recently been defined.¹ These criteria include both the rapid release of the biomarker into the blood for early detection and prolonged elevation for later assessment and confirmation. Additionally, the quantitative assay must possess a high clinical sensitivity and specificity. The American College of Cardiology (ACC) and the American Heart Association (AHA) currently recognize a biomarker panel composed of myoglobin, cardiac troponin I (cTnI), and creatine kinase MB (CK-MB) for the diagnosis of AMI.^{2,3} However, because CK-MB has a low sensitivity for AMI within six hours after an incident and cTnI is better at detecting minor cardiac damage, CK-MB was not evaluated in this study.² Instead, heart-type fatty acid binding protein (H-FABP) was included due to its early release following cardiac injury and diagnostic potential when used as part of a panel with cTnI.⁴⁻⁷

Myoglobin is an oxygen-binding protein found in both cardiac and striated muscle, and is currently used as a routine biomarker for AMI.^{8,9} Its early release into the blood (increasing 1-3 hours within the onset of myocardial necrosis), as well as relatively high plasma reference concentration (34 $\mu\text{g/L}$) illustrate several of the qualities desired in an ideal cardiac marker.⁹ However, because it may also indicate skeletal muscle damage, by itself myoglobin has shown a sensitivity of 75.9%, and a clinical specificity of only 25.0% for AMI diagnosis. In recent years H-FABP has also shown promise as an early cardiac injury marker in plasma.^{4,7,10,11} Due to its lower concentration in skeletal muscle compared to myoglobin, rapid release into circulation,

1
2
3 and potential to predict patient prognosis, H-FABP has received considerable attention.^{5-7,12,13}
4 Still, because of its release in other medical conditions, H-FABP alone shows only a 64%
5 sensitivity.^{5,14} While no single marker has shown adequate diagnostic accuracy for AMI, a high
6 sensitivity and specificity has been achieved using myoglobin and H-FABP as part of a
7 biomarker panel along with cTnI.^{5,8,10,12,14-16} Even with the use of biomarker panels, there exists a
8 need for more sensitive assays capable of rapid analysis for the evaluation of serial
9 measurements to be practical in a clinical setting. This capability would be beneficial not only in
10 the diagnosis of AMI, but for the early detection of many diseases which could greatly improve
11 prognoses.
12

13
14
15 Over the last few years a great deal of research has been devoted to the development of
16 micro-immunoassay platforms allowing for the sensitive quantitation of varied target
17 biomarkers.¹⁷⁻²⁵ A particularly interesting subset of this research incorporates the use of magnetic
18 micro- or nano-particles as the solid surface employed for primary antibody fixation and target
19 trapping.²⁶⁻³⁴ Use of magnetic particles permits easy sample manipulation and separation from
20 interfering species, as well as straightforward coupling to signal amplification and signal
21 processing.
22

23
24
25 This work describes the development of a micro-immunoassay platform that allows
26 extremely sensitive quantitation. Unique to this technique among magnetic microbead
27 immunoassays is the manipulation of the solid capture surface during data capture. Incorporation
28 of a periodic fluctuation into the observed fluorescence aids in the identification and
29 quantification of the specific signal. This reduces the impact of background fluorescence on
30 quantitative abilities and enables increased sensitivity compared to previous results. This system
31 directly and indirectly addresses many the six metrics of an optimized immunoassay: increased
32 sensitivity, reduced analysis time, reduced cost, lower sample volumes, ability to multiplex and
33 operational simplicity.³⁵ This work has focused on the optimization of assay features enabling
34 high quantitative sensitivity using small sample volumes and the first steps toward multiplexed
35 detection. Analysis times have been reduced and could be shortened further through
36 incorporation onto a microdevice. Through clinical samples have not yet been evaluated using
37 this technique, these samples cannot effectively be tested until the improvements to the metrics
38 of an optimized assay addressed in this work have been achieved. While the studies here are
39 performed on an AMI biomarker panel composed of myoglobin, cTnI and H-FABP, this format
40 is easily adaptable to the detection of limitless targets and may be incorporated as a detection
41 method into a micro-total analysis system (μ TAS) for the parallel detection and quantification of
42 biomarker panels.
43
44
45
46
47
48
49

50 51 **Experimental**

52 **Myoglobin Detection Antibody Conjugation to Fluorescein-5-EX, Succinimidyl Ester**

53
54
55 Fifty micrograms (50 μ L; 1 mg/mL) of polyclonal rabbit anti-human myoglobin reconstituted in
56 DI H₂O (LSBio, Seattle, Washington) was added to 50 μ L of 1 M sodium bicarbonate in a 1.5
57
58
59
60

1
2
3 mL capped vial. One milligram of fluorescein-5-EX, succinimidyl ester (FEXS, Invitrogen) was
4 dissolved in 0.1 mL dimethyl sulfoxide (DMSO) and added dropwise to the polyclonal antibody
5 (Pab) solution at room temperature. This was reacted in darkness at room temperature for 3 hours
6 on a stir plate (Corning) and then placed at 4°C to continue the reaction overnight. The crude
7 reaction mixture was added to a purification column with a 15,000 Dalton molecular weight cut-
8 off (Invitrogen). The fluorescently labeled antibody was separated on-column from unbound dye
9 using 10 mM PBS with 0.15 M NaCl and 0.2 mM NaN₃, pH 7.2 and collected in a single
10 fraction. The purified FEXS-Pab solution was analyzed for absorbance measurements at 280 and
11 494 nm (BioTeck Synergy HT Multi-Mode Microplate Reader). These measurements were used
12 to determine the quantity of antibody present and extent of FEXS conjugation.³⁶
13
14
15
16
17

18 **cTnI and H-FABP Detection Antibody Conjugation to NHS-Fluorescein**

19
20 For the detection of cTnI and H-FABP, 250 µg (250 µL; 1 mg/mL) of polyclonal goat anti-
21 human cTnI and 100 µg (100 µL; 1 mg/mL) polyclonal rabbit anti-human FABP were used as
22 purchased in PBS buffer (cTnI: 0.1% NaN₃; FABP: 0.02% NaN₃, 0.1% BSA), pH 7.2. NHS-
23 Fluorescein (Thermo Scientific) was dissolved in DMSO to a concentration of 10 mg/mL and
24 added dropwise to the Pab solutions at room temperature (24 µL and 40 µL, respectively). This
25 was reacted in darkness at room temperature for two hours on a shaker (Southwest Science
26 LabMini MiniMixer). The crude reaction mixtures were added to dialysis cups (Thermo
27 Scientific) with a molecular weight cut-off of 3,500 Daltons. The labeled protein was dialyzed in
28 100 mM PBS with 0.02% NaN₃ and 0.1% Tween 20, pH 7.2 overnight. The dialyzed NHS-
29 Fluorescein-Pab solutions were analyzed for absorbance measurements utilizing the same
30 method as for anti-human myoglobin Pab.
31
32
33
34
35

36 **Preparation of Capture Antibody and Particles**

37
38 Biotinylated anti-myoglobin monoclonal antibody (bMab; 100 µL; 1.4 mg/mL; LSBio) was
39 incubated with 3 µL of BioMag paramagnetic particles having an average diameter of 1.6 µm
40 and ranging in diameter from 1.0-2.0 µm (Quagen, Inc.). The total reaction volume was diluted
41 to 300 µL with PBS at pH 7.2 containing 5% BSA, 0.1% Tween-20, and 0.1% NaN₃. This was
42 incubated for 3 hours on a shaker (Southwest Science LabMini MiniMixer) at room temperature
43 and then stored at 4°C until used. Biotinylated anti-cTnI Mab (50 µL, 2 mg/mL, LSBio) and
44 biotinylated anti-FABP Mab (45 µL, 2.33 mg/mL, LSBio) were prepared in the same way.
45
46
47
48

49 **Sandwich Immunoassays**

50
51 Purified human myoglobin (7.33 mg/mL) was purchased from MyBioSource, LLC (San Diego,
52 California). Standards ranging in concentration from 0.62 fg/mL to 25 ng/mL (36 aM to 1.5 nM)
53 were created in buffer through serial dilution of the stock myoglobin. Following sample
54 preparation 30 µL of each Mb standard was mixed with 30 µL of the bMab-BioMag colloid and
55 5% BSA to prevent non-specific binding. Samples were incubated at room temperature on a
56
57
58
59
60

1
2
3 shaker for 1 hour. Following the incubation, 4 μL of the detection polyclonal antibody-FEXS
4 solution was added to each sample and incubated in the dark at room temperature for 1 hour with
5 shaking. After the incubation, samples were washed 3 times using 60 μL of PBS buffer and then
6 exchanged to a final volume of 30 μL . Three separate 10 μL droplets were analyzed for each
7 sample, with a total of ten analyses performed for each concentration. Purified human cTnI (1.07
8 mg/mL) and H-FABP (2.2 mg/mL) were purchased from Life Diagnostics (West Chester,
9 Pennsylvania). Standards ranging in concentration from 10 fg/mL to 10 ng/mL (0.42 fM to 0.42
10 nM) for cTnI and from 1 fg/mL to 10 ng/mL (67 aM to 0.67 nM) for H-FABP through serial
11 dilution of the initial stock solutions. Following sample preparation samples were prepared and
12 analyzed in the same way as myoglobin.
13
14
15
16

17 **Data Collection**

18
19
20 Data were collected using an Olympus IX70 inverted microscope with a charge coupled device
21 (CCD) camera connected to a computer capable of image-capture (Q-Imaging, Surrey, BC).
22 Capture settings for the CCD camera were optimized for the observation of strong fluorescent
23 signal clusters with minimal contribution from background pixels through studies utilizing
24 biotinylated fluorescein (Sigma-Aldrich) as a positive control. Biotinylated fluorescein was
25 chosen as a control due to the strong binding relationship between biotin and the streptavidin on
26 the BioMag particles and a common fluorophore with the experimental immunoassays. Offset
27 was adjusted to minimize background of a washed sample without reducing pixel intensity from
28 signal; values between -1120 to 440 were tested. With the offset held constant at 100 , gain
29 values between 4.7 to 15.0 were explored to maximize the sensitivity of the assay without
30 compromising the dynamic range. Optimal image quality was observed at an offset of 100 and
31 gain of 13.8 . Once established, capture settings were held constant for all experiments performed
32 on cardiac targets.
33
34
35
36
37

38 Multiple 10 μL -sized droplets were analyzed for each sample concentration using a
39 microscope slide having a small hydrophilic zone encompassed by a hydrophobic Teflon coating
40 (Tekdon Inc., Myakka City, Florida). A cylindrical rare earth magnet (2.5 cm diameter, 0.3 cm
41 thick) placed 2 cm above the droplet was used to generate the magnetic field (Magcraft, Vienna,
42 VA) and collect structures for ~ 30 s. Supraparticle structures approximately 15 μm in length were
43 observed. The magnet was secured to a DC motor by a 7 cm metal shaft allowing for rotation
44 and controlled via a USB 4-motor stepper controller (Trossen Robotics). The controller was
45 connected to the motor through a ribbon wire to protect it from fluids used during the
46 experiment. The magnet was rotated at a constant velocity during assays (30 rpm), and
47 illumination from a mercury lamp (Olympus) was passed through the appropriate filter cube and
48 a LCPlanFl 40X/0.60 objective to excite the assay. Emitted fluorescence was collected using the
49 QIACAM FAST cooled Mono 12-bit (QImaging) CCD camera and stored as video files.
50
51
52
53
54

55 **Data Analysis**

1
2
3 Video was analyzed using Image J (National Institute of Health, Bethesda, Maryland). The
4 images (492 x 396) were captured at an exposure time of ~120 ms (gain, 13.8; offset, 100) which
5 translates to a rate of ~12 frames/s. Fluorescence intensity measurements were collected by
6 manually selecting all rotors (regions of interest, ROI) within a video frame and summing the
7 fluorescence intensity. This was performed for ten randomized frames per video and the resulting
8 intensities were averaged to attain a single average fluorescence intensity value for a given trial.
9 Ten trials per sample concentration were averaged per experiment.

13 **Results/Discussion**

14 **Assay Optimization and Protein Detection**

15
16
17 Three human cardiac biomarkers, myoglobin, cTnI, and H-FABP, were quantified in buffer
18 using a singleplex immunoassay detection system. Proteins were detected by adjusting the
19 hardware settings such that images with visible, yet unsaturated, signal clusters with minimal
20 background contribution were captured. Using an exposure time of 120 ms, signals generated
21 from low concentrations of proteins (down to 36 aM of myoglobin) were detected above the
22 background intensity (Figure 1).
23
24
25

26 Control experiments were performed at a zero antigen concentration, exposing
27 paramagnetic particles with immobilized capture antibody to fluorescently-labeled detection
28 antibody. Dark structures resulted, with minimal diffuse fluorescence suggesting that little or no
29 nonspecific binding is present. The average fluorescence intensity of the entire image was noted
30 (including pixels from all areas, including diffuse fluorescence between rotors) since distinct
31 signal clusters were not visible. This is a more stringent test for background quantification, since
32 the noise from all pixels is included.
33
34
35

36 At low sample concentrations, below 360 aM for myoglobin, the signal becomes highly
37 variable and the uncertainty in the measurements was greater than 10%. When the uncertainty in
38 a measurement rises above 10% the signal be detected, but not quantified with a reasonable level
39 of certainty.³⁷ This distinction is important as it differentiates a qualitative positive result from
40 the ability to distinguish when a biomarker is present in concentrations that correspond to
41 diagnostic cut-off values. For the optimization of a clinical assay it is the quantitation limit that is
42 of interest.
43
44
45
46
47
48
49
50
51
52
53
54
55
56
57
58
59
60

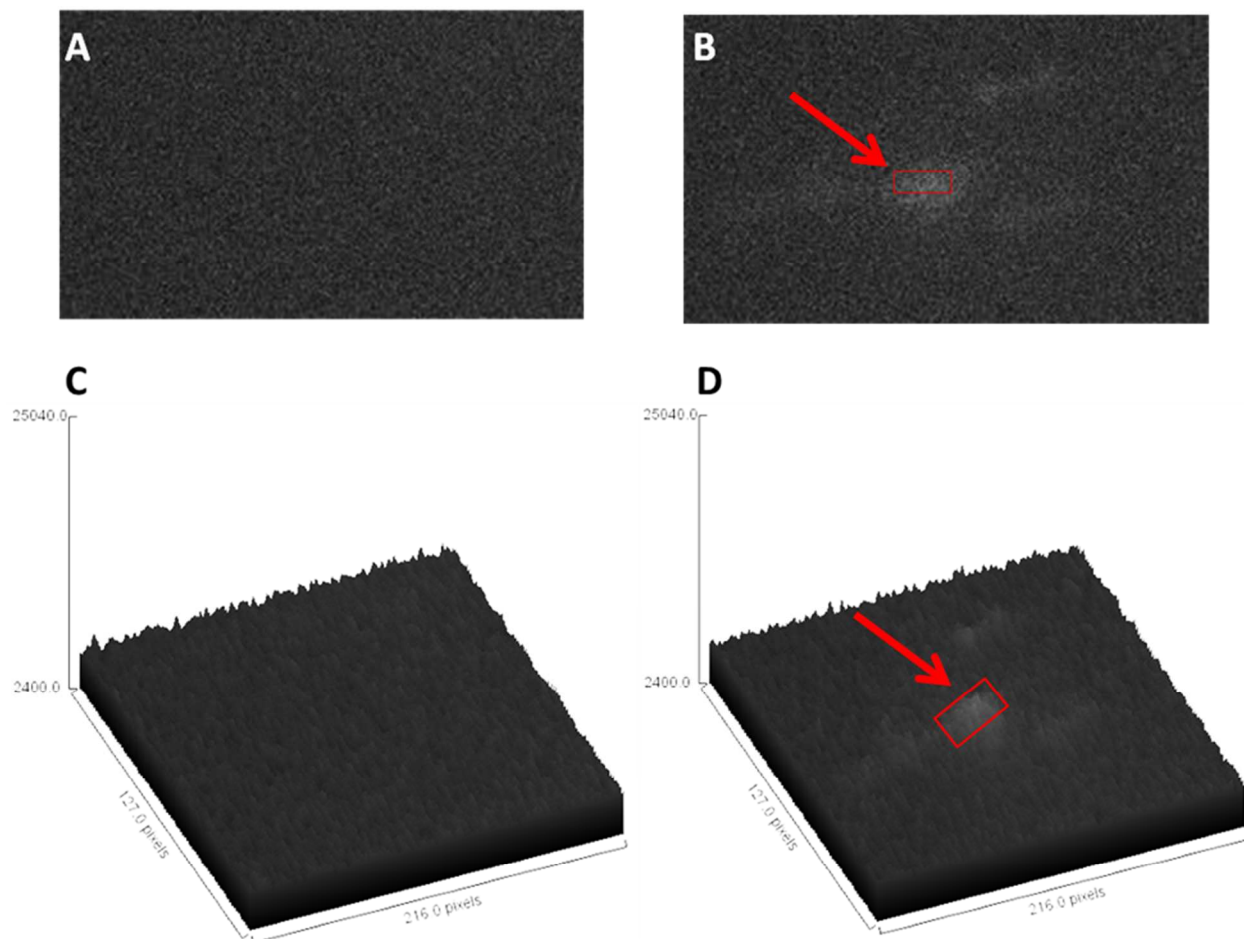


Figure 1 (A and B) Images showing fluorescence of high sensitivity immunoassays at the detection limit (below the limit of quantification) for 36 aM myoglobin (**B**) compared to background (**A**). (**C and D**) Surface plots illustrating the difference in fluorescence intensity between background (zero concentration, **C**) and signal clusters representing specific signal (36 aM myoglobin, **D**). While the signal clusters are not as distinct as those observed for higher target concentrations, this represents the lower limit detectable above zero concentration. Red boxes and arrows indicate the position of the observed signal above background.

Quantitation Limit

Measurements of cardiac targets permitted the quantitation of myoglobin to a minimal concentration of 360 ± 2.5 aM with an observed detection limit of 36 ± 2.5 aM, and a linear standard curve from 360 aM to 14 fM ($R^2 = 0.996$; Fig. 2A). H-FABP and cTnI were quantified to limits of 67 ± 3 fM and 42 ± 0.01 fM, with linear standard curves from 67 fM to 67 pM and 42 fM to 42 pM, respectively ($R^2 = 0.998$; Fig. 2B and $R^2 = 1$; Fig. 2C). The optimized collection of the video sets allowed for improvement in detection over several orders of magnitude compared to previously collected myoglobin data, from 50 pM to 36 aM (Table 1).³⁰ In addition to approaching these fundamental limits of quantification, the linear range of this method may be easily scaled for the detection of higher concentration samples through the addition of more

magnetic microparticles or through sample dilution. The limits of quantitation observed in the present work compare favorably to the metrics of a fully optimized immunoassay, achieving detection on the same order of magnitude as fundamental limitations. At low numbers of molecules, quantification becomes impossible due to Poisson statistics.³⁷ While targets may be observed below this limit, they may not be quantified due to high levels of uncertainty in the measurements made.

| | Previous Studies ³⁰ | Commercial Techniques ^{38,39} | Present Work | Optimized Values | Plasma Concentration ⁴⁰ |
|-----------|---------------------------------------|---|---------------------|-------------------------|---|
| Myoglobin | 50 pM | 1.5 nM | 360 ± 2.5 aM | 33 aM | 2.5 nM |
| H-FABP | -- | 6.7 pM | 67 ± 3 fM | 33 aM | 110 pM |
| cTnI | -- | 83 pM | 42 ± 0.01 fM | 33 aM | 62.5 pM |

Table 1 Quantitation limits for immunoassay techniques. Optimized values represent the limit to immunoassay quantitation in a 10 μ L sample volume.

Several differences exist in both the data acquisition and data analysis performed in this work that account for the observed improvement in quantitation ability compared to previous studies.³⁰ In terms of data acquisition, previous work noted differences in signal strength depending on their location in the field of view, increasing variation in both signal and noise. The changes to optics and acquisition conditions eliminated this issue, producing rotors with similar signal intensities independent of their location. Optimizing acquisition conditions through control studies with b-Fluorescein resulted in an increase in exposure time from 50 to 120 ms, as well as reductions in gain (from 2000 to 13.8) and offset (from 2600 to 100).³⁰ The increase in exposure time still allowed clear visualization of rotor rotation while reducing the impact on noise compared with a shorter exposure. With a lowered gain, the amplification of the image collected by the CCD camera is reduced. Since both the signal and noise are reduced, this lowered value will improve the signal-to-noise ratio (S/N) and reduce the background intensity and noise while specific signal remains visible. By contrast, reducing the offset allows lower intensity values for both specific signal and background fluorescence to be captured. While this increases both the background intensity and noise as well as signal intensity and noise, this minimal value assures that clusters from low signal concentrations may be observed. By improving the signal-to-noise ratio of the captured video files lower intensity signals may be differentiated from background noise, improving assay sensitivity.

Along with the changes made to data acquisition conditions, the process of data analysis has also been altered to increase the signal power obtained from each sample.³⁰ In previous work a small region of each image (150 x 120 pixels), containing roughly two of the 10-15 signal clusters present overall, was analyzed. Additionally, while signal clusters contributed to less than 30% of the region selected, the average pixel intensity was calculated for the entire selected area, including both signal and noise.⁴¹ Signal processing studies performed on this data conclude that

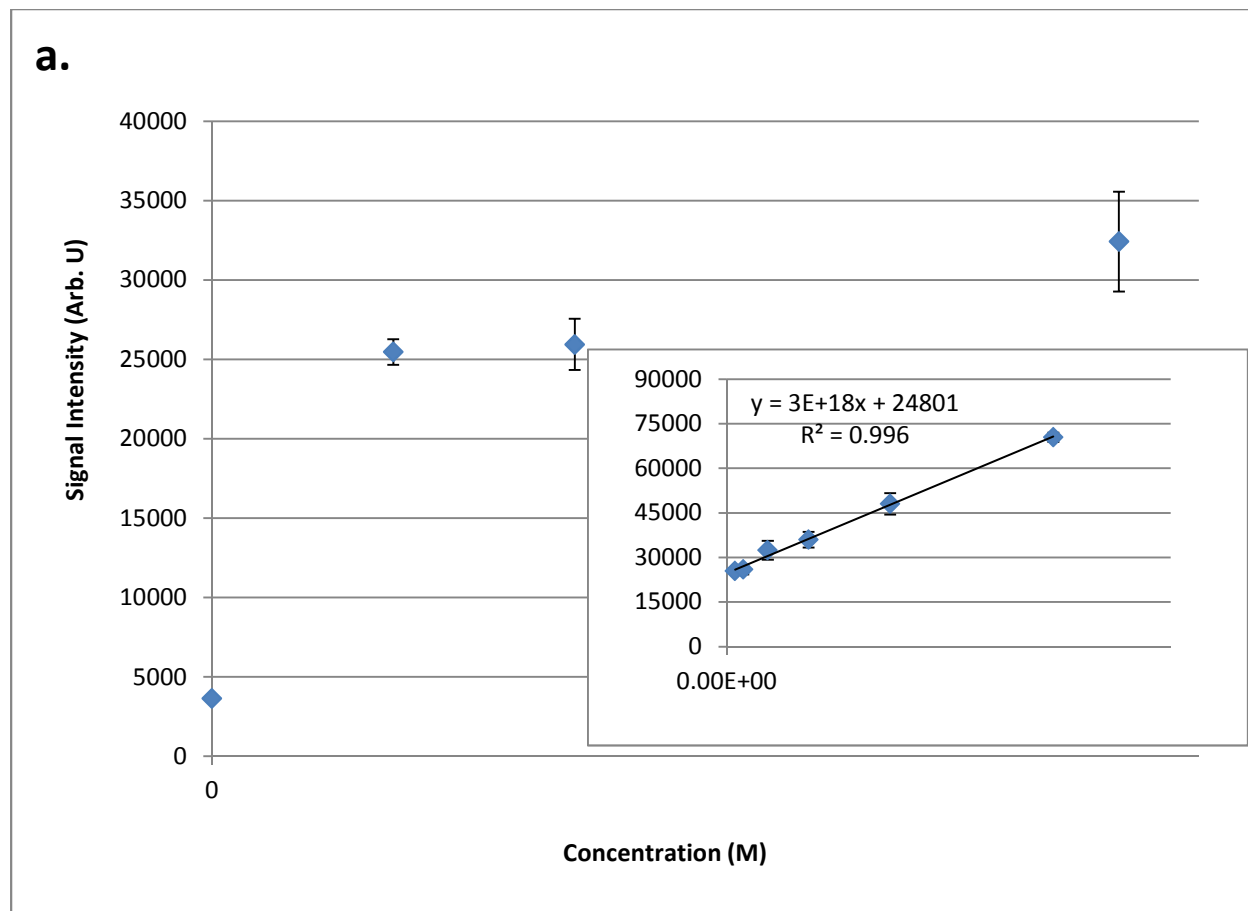
1
2
3 by calculating pixel intensity for the entire image selection, and by only two of the signal clusters
4 contributing to target quantification, a large portion of the signal power is lost while the noise
5 power is increased.⁴¹ By manually segmenting data and selecting all rotors in each frame (492 x
6 396 pixels) as was done in this work, both issues observed with previous analysis methods are
7 solved. The overall noise power is reduced while signal power is increased.⁴¹ This, coupled to
8 the increase in S/N through optimal data acquisition conditions, allowed for a five-fold
9 improvement in assay sensitivity.

10
11 In terms of the mass action equilibrium and detection, sensitivity is maximized by using
12 an excess of both primary and secondary antibodies, and heavy labeling of secondary antibodies
13 (average among all targets of 4 labels per antibody). Given that the paramagnetic particles have a
14 binding capacity of 8.2 nmol/mL (manufacturer specifications), the binding capacity for the
15 primary antibody preparation is 82 nM. Using fundamental relationships from basic
16 immunology, the equilibrium reaction between the protein and primary antibody can be
17 described as

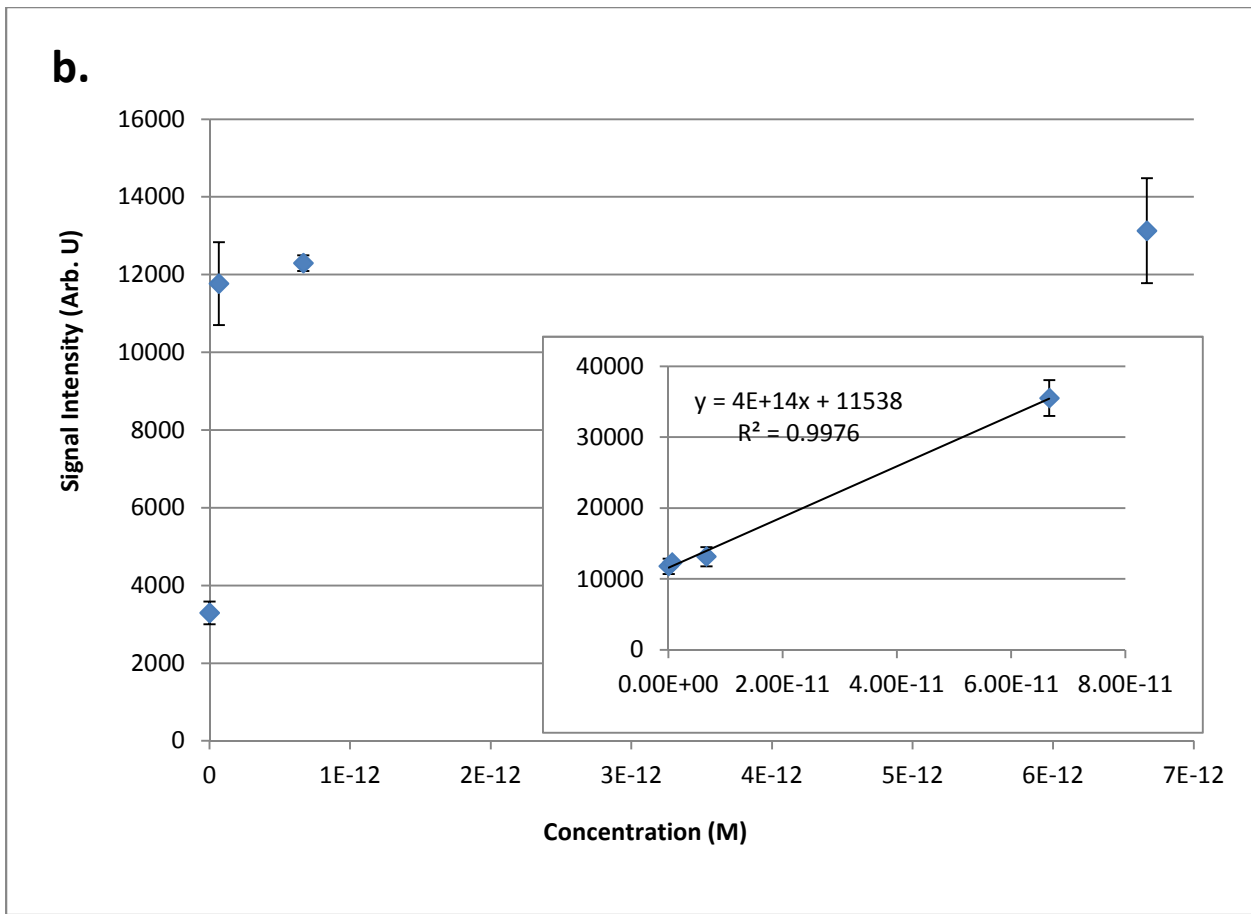
$$K_{eq} = \frac{[AgAb1]}{[Ag][Ab1]} \quad (1)$$

18
19 where $[AgAb1]$ is the concentration of bound antigen, $[Ag]$ is the concentration of antigen, $[Ab1]$
20 is the concentration of primary antibody, and K_{eq} is the equilibrium constant. Given a K_{eq} of 10^9
21 M^{-1} , the equilibrium concentration of bound antigen for a myoglobin sample at a concentration
22 of 3.6 fM is 0.3 pM, about one hundred times the concentration of target present. A similar
23 calculation can be performed for the reaction of bound antigen with secondary antibody, giving
24 an equilibrium concentration of $[AgAb2]$ in the nM range. With these experimental conditions it
25 can be determined that nearly all antigen is bound in the sandwich immunoassay, resulting in a
26 linear response for the portion of the sigmoidal immunoassay curve examined.

27
28 At myoglobin concentrations below 360 aM, uncertainty is too high in the measurement
29 to achieve satisfactory quantitation. Although the lowest concentrations detected could not be
30 quantified due to high variations in signal, the potential exists to improve quantitative sensitivity
31 through coupling to available signal processing approaches.⁴¹ Using this approach, the detection
32 limit of previously published data has been improved by a factor of 100. If the same factor of
33 improvement and reduction in uncertainty for a given sample was realized for the data collected
34 in this work, quantitation of the lowest sample data collected would be possible.

1
2
3
4
5
6
7
8
9
10
11
12
13
14
15
16
17
18
19
20
21
22
23
24
25
26
27
28
29
30
31
32
33
34
35
36
37
38
39
40
41
42
43
44
45
46
47
48
49
50
51
52
53
54
55
56
57
58
59
60

1
2
3
4
5
6
7
8
9
10
11
12
13
14
15
16
17
18
19
20
21
22
23
24
25
26
27
28
29
30
31
32
33
34
35
36
37
38
39
40
41
42
43
44
45
46
47
48
49
50
51
52
53
54
55
56
57
58
59
60



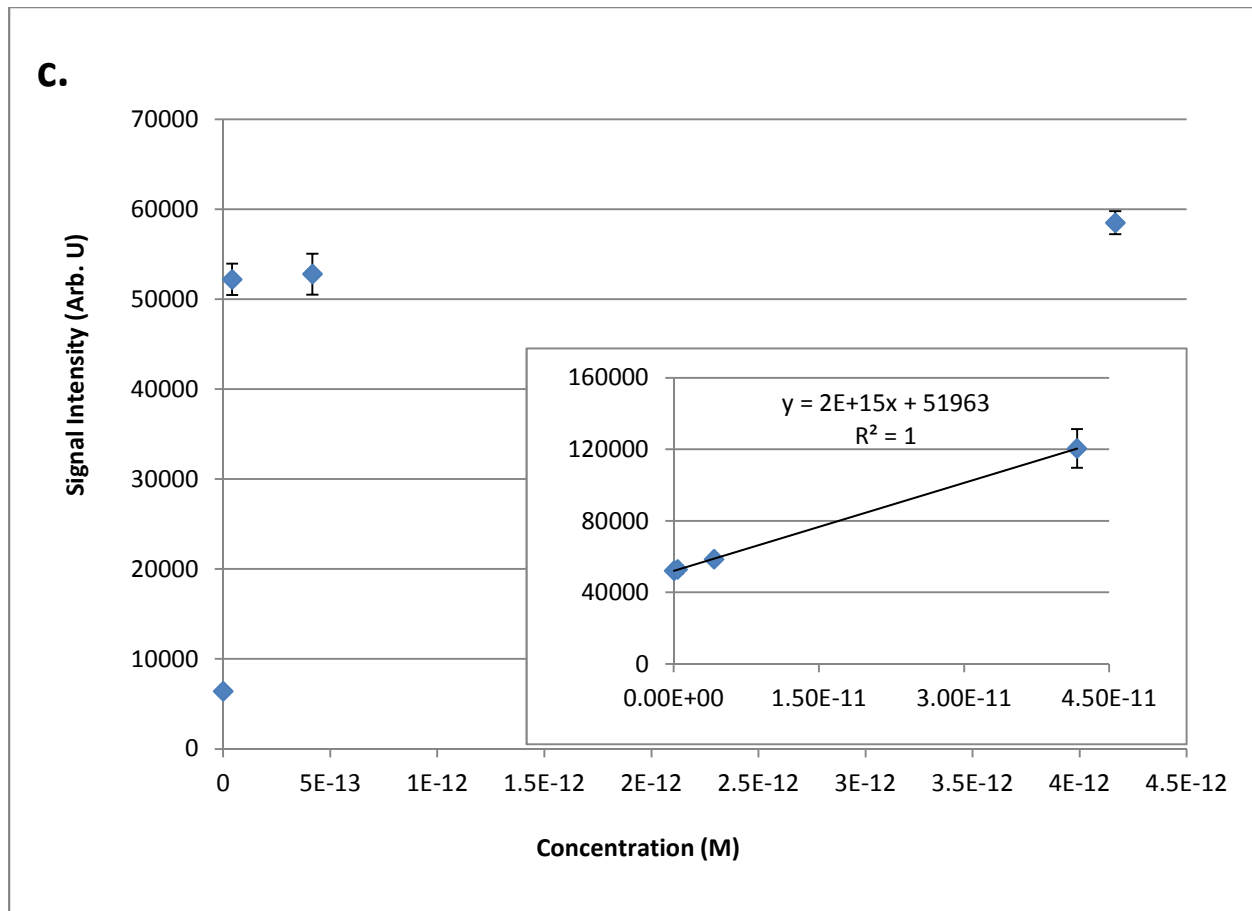


Figure 2 Standard curves showing signal intensity data for the sandwich immunoassays performed on cardiac biomarker targets. **a.** Plot showing the quantitation of Myoglobin down to a minimal concentration of 360 aM. Inset shows the linear range to 14.7 fM. **b.** Plot showing the quantitation of h-FABP to a minimal concentration of 67 fM with inset showing the linear range to 67 pM. **c.** Plot showing the quantitation of cTnI to a minimal concentration of 42 fM with inset showing the linear range to 42 pM.

Repeated experiments exhibit a similar result. Figure 3 shows the average fluorescence intensity of data collected from four separate experiments with independent dilutions of a myoglobin stock sample. Error bars show the standard deviation of each data set. Differences in overall fluorescence intensity were observed between experiments, due to aging of the mercury lamp used to illuminate samples. Even when differences in fluorescence intensity were observed between days, the same linear relationship was observed.

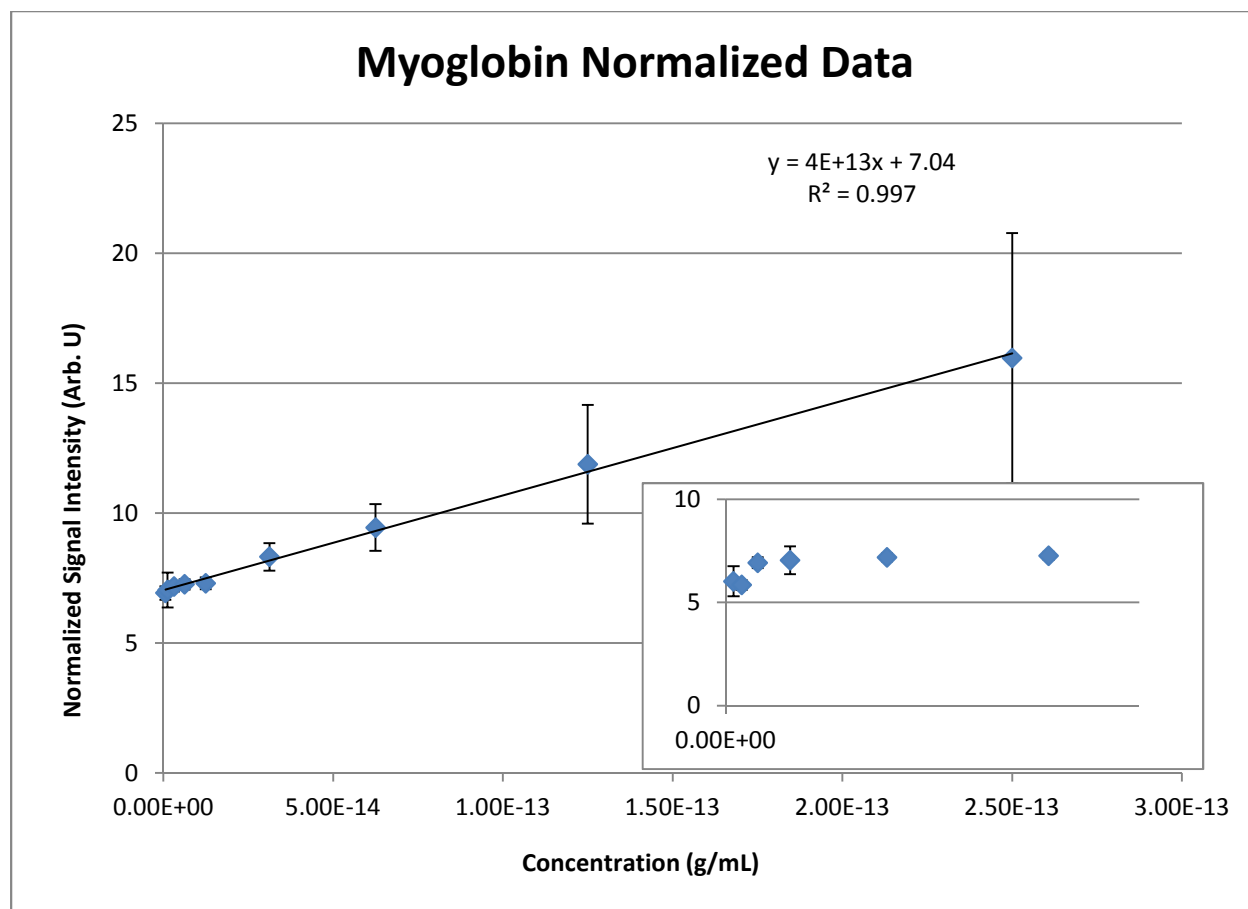


Figure 3 Standard curve showing the average signal intensity versus concentration for the myoglobin sandwich immunoassay for four different experiments using the target protein. The inset shows the lower concentrations on the standard curve, error bars represent the standard deviation among data sets. Signal intensity has been normalized to the background intensity (zero concentration) for each data set.

Assay Evaluation

As has been noted previously, in static immunoassays background fluorescence is a serious concern that limits the ability to differentiate specific signal from noise. Signal processing strategies offer the potential to improve detection limits through the identification of specific signal generating surfaces and reduction of background elements to reduce the variation observed in signal intensity for low concentration samples.⁴¹ Surface localization is of use in image processing because it creates distinct signal objects that are easier to detect and quantify compared to signal spread over the entire field of view. Creating these distinct signal objects allows for segmentation of collected images and the quantitation of fluorescent species bound in the immunoassay without the influence of diffuse background fluorescence.

The potential to optimize quantitation capabilities also exists through the use of new signal input patterns. Lock-in amplification is a commonly employed method to recognize a specific input signal in the presence of noise.⁴² This method allows an input signal modulated in

1
2
3 amplitude to be matched to a reference signal with the same periodicity and amplified while
4 background noise is not recognized and is effectively removed. It has been used in previous work
5 to achieve detection limits in the pM range.^{30,32} However, because the reference signal generated
6 by lock-in amplification is a sine wave, its correlation with the input wave is imperfect and
7 signal power is lost. This has been addressed in part by the development of a new signal
8 processing method that maintains the input signal modulation but uses a new waveform as the
9 reference signal.³⁷ While this approach was successful in improving quantitation, using
10 autocorrelation analysis to recognize more complicated input patterns could improve the
11 distinction between signal and noise and increase the slope of the regression line at low sample
12 concentrations.
13
14
15
16

17 Other immunoassay techniques have worked on improving quantitative sensitivity for
18 protein targets.^{17,23-25,33,34} Compared to those studies that were performed using traditional
19 laboratory equipment,^{23-25,33,34} the assay investigated in this work achieved superior sensitivity
20 (aM to fM range compared with typical nM sensitivity) using shorter incubation times. Another
21 study discussed the development of a microchip-based immunoassay for cTnI detection.¹⁷
22 Movement to the chip format allowed for shorter analysis times and easy adaptability to portable
23 devices and multiplexed analysis. While offering an improvement over this work in terms of
24 analysis time, the sensitivity achieved in this work was superior (fM compared with pM) using a
25 comparable sample volume.
26
27
28

29 The three biomarker targets evaluated in this work present clinically at levels in the pM-
30 nM range (Table 1).⁴⁰ As tested in this work, superior levels of sensitivity, beyond those
31 necessary for clinical diagnostics have been achieved. Testing of increasingly complex samples
32 in plasma or from whole blood could introduce additional matrix effects influencing various
33 aspects of the assay. While additional refinement of the platform may be necessary, achieving
34 high sensitivity in a buffer system represents a necessary first step in an optimized assay design.
35
36
37

38 Many studies have reported on the improved sensitivity of cardiac diagnostic ability with
39 the use of a biomarker panel as opposed to a single target.^{5,8,10,12,14-16} One consequence of this is
40 that parallel detection of targets from a single sample is desirable. Along with the potential to
41 optimize this immunoassay platform for sensitive analyte quantitation, the use of magnetic
42 microparticles offers the ability to move from the batch incubation assay conducted within this
43 work to one performed on a microchip as part of a total sample analysis system. Movement to a
44 microchip would allow the remaining metrics of an optimized immunoassay to be directly
45 addressed. Easy manipulation of the magnetic solid surface through an applied magnetic field
46 allows for the containment of surfaces functionalized for the capture of different targets in
47 separate regions of the microchip. Following target isolation on chip through separation science
48 techniques, individual species may be flushed into appropriate detection chambers and
49 quantified. Use of convective mixing through the manipulation of the microbead surface could
50 aid in rapid analyte capture and greatly reduce analysis times. The linear range of this technique
51 may also be extended through the dilution of samples investigated, or use of smaller sample
52
53
54
55
56
57
58
59
60

volumes, allowing the assay to be tailored to meet detection needs as required for diagnostic or disease monitoring purposes.

Conclusions

Dispersed magnetic beads were utilized in a batch incubation format to conduct sandwich immunoassays on three cardiac biomarker targets. Following sample preparation, 10 μ L droplets were manipulated through variations in an applied magnetic field, and the periodic change in observed fluorescence was captured as a video file. Analysis of video utilizing ImageJ allowed the superior detection of myoglobin (360 aM), H-FABP (67 fM) and cTnI (42 fM) compared to previous results. Though not tested using clinical samples, where matrix effects may impact assay features and necessitate additional optimization, this work represents a necessary first step in the design, evaluation and optimization of an immunoassay platform capable of optimized clinical testing. Improvements to the many of the metrics required for an optimized immunoassay have been achieved in this work, and future studies will allow the remaining features to be directly addressed.

Thus, a magnetic bead immunoassay platform was demonstrated utilizing simple batch incubation and a modified microscope slide. This platform has the potential to be incorporated into a full sample analysis chip as a quantification method for biomarker panels while maintaining sensitive detection capabilities, and offers the ability to couple results to more sophisticated signal processing approaches for the detection of low sample concentrations independently from background noise. In its current form this system directly addresses many of the six metrics of an optimized immunoassay. Incorporation of the assay into a μ TAS could further these efforts by affording the ability to multiplex and reduce analysis times while maintaining the high sensitivity, low sample volume, and operational simplicity achieved herein.

Acknowledgements

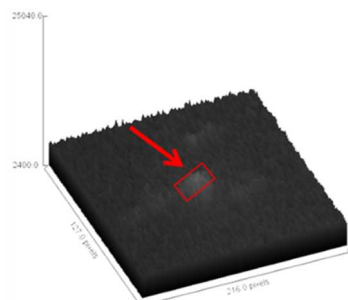
This work was supported by National Institutes of Health grant 5R21EB010191-02.

References

- 1 A. Qureshi, Y. Gurbuz, J.H. Niazi, *Sensors and Actuators B*, 2012, **171-172**, 62-76.
- 2 ACC and Cardiac Biomarkers, 2014, <http://www.acc.org/education-and-meetings/image-and-slide-gallery/media-detail?id=d9c880ce33f3482f993161076a32990a>
- 3 R. S. Vasan, *Circulation*, 2006, **113**, 2335-2362.
- 4 A. Kakoti, P. Goswami, *Biosensors and Bioelectronics*, 2013, **43**, 400-411.
- 5 J. Ishii, J.H. Wang, H. Naruse, S. Taga, M. Kinoshita, H. Kurokawa, M. Iwase, T. Kondo, M. Nomura, Y. Nagamura, Y. Watanabe, H. Hishida, T. Tanaka, K. Kawamura, *Clinical Chemistry*, 1997, **43**, 1372-1378.
- 6 C.H. Huang, M.S. Tsai, K.L. Chien, C.Y. Hsu, W.T. Chang, T.D. Wang, S.C. Chen, M. Huei-Ming Ma, W.J. Chen, *Clinica Chimica Acta*, 2014, **435**, 7-13.

- 1
2
3
4
5
6
7
8
9
10
11
12
13
14
15
16
17
18
19
20
21
22
23
24
25
26
27
28
29
30
31
32
33
34
35
36
37
38
39
40
41
42
43
44
45
46
47
48
49
50
51
52
53
54
55
56
57
58
59
60
- 7 J.F. Glatz and R. Renneberg, *Clinical Lipidology*, 2014, **9**, 205-220.
 - 8 S.P.J. Macdonald, Y. Nagree, D.M. Fatovich, M. Phillips, S.G.A. Brown, *Emergency Medicine Journal*, 2012, **30**, 149-154.
 - 9 J. Liao, C.P. Chan, Y. Cheung, J. Lu, Y. Luo, G.W.H. Cauterley, J.F.C. Glatz, R. Renneberg, *International Journal of Cardiology*, 2008, **133**, 420-423.
 - 10 Y. Tonomura, S. Matsushima, E. Kashiwagi, K. Fujisawa, S. Takagi, Y. Nishimura, R. Fukushima, M. Torii, M. Matsubara, *Toxicology*, 2012, **302**, 179-189.
 - 11 K. Inoue, S. Suwa, H. Ohta, S. Itoh, S. Maruyama, N. Masuda, M. Sugita, H. Daida, *Circulation Journal*, 2011, **75**, 2813-2820.
 - 12 S.Da. Molin, F. Cappellini, R. Falbo, S. Signorini, P. Brambilla, *Clinical Biochemistry*, 2014, **47**, 247-249.
 - 13 K. Setsuta, Y. Seino, K. Mizuno, *International Journal of Cardiology*, 2014, **176**, 1323-1325.
 - 14 C.G. McMahon, J.V. Lamont, E. Curtin, R.I. McConnell, M. Crockard, M.J. Kurth, P. Crean, S.P. Fitzgerald, *American Journal of Emergency Medicine*, 2012, **30**, 267-274.
 - 15 O.V. Gnedenko, Y.V. Mezentsev, A.A. Molnar, A.V. Lisitsa, A.S. Ivanov, A.I. Archakov, *Analytica Chimica Acta*, 2013, **759**, 105-109.
 - 16 R. Body, G. McDowell, S. Carley, C. Wibberley, J. Ferguson, K. Mackway-Jones, *Resuscitation*, 2011, **82**, 1041-1046.
 - 17 S. Y. Song, Y. D. Han, K. Kim, S. S. Yang, and H. C. Yoon, *Biosensors and Bioelectronics*, 2011, **26**, 3818-3824.
 - 18 S. Casolari, B. Roda, M. Mirasoli, M. Zangheri, D. Patrono, P. Reschiglian, and A. Roda, *Analyst*, 2013, **138**, 211-219.
 - 19 J. Tian, L. Zhou, Y. Zhao, Y. Wang, Y. Peng, X. Hong, S. Zhao, *J Fluoresc*, 2012.
 - 20 D. Lin, J. Wu, M. Wang, F. Yan, and H. Ju, *Analytical Chemistry*, 2012, **84**, 3662-3668.
 - 21 G. Liang, S. Liu, G. Zou, and X. Zhang, *Analytical Chemistry*, 2012, **84**, 10645-10649.
 - 22 S. Spindel and K.E. Sapsford, *Sensors*, 2014, **14**, 22313-22341.
 - 23 M. Ammar, C. Smadja, G.T. Phuong, M. Azzous, J. Vigneron, A. Etcheberry, M. Taverna, E. Dufour-Gergam, *Biosensors and Bioelectronics*, 2013, **40**, 329-335.
 - 24 M.M. Caulum, B.M. Murphy, L.M. Ramsay, C.S. Henry, *Analytical Chemistry*, 2007, **79**, 5249-5256.
 - 25 M. Park, J.H. Bong, Y.W. Chang, G. Yoo, J. Jose, M.J. Kang, J.C. Pyun, *Analytical Methods*, 2014, **6**, 1700-1708.
 - 26 J. Han, J. Zhang, Y. Xia, S. Li, and L. Jiang *Colloids and Surfaces A: Physiochem. Eng. Aspects*, 2011, **379**, 2-9.
 - 27 G. Proczek, A. L. Gassner, J. M. Busnel, and H. H. Girault *Anal. Bioanal. Chem.*, 2012, **402**, 2645-2653.
 - 28 A. Ranzoni, G. Sabatte, L. J. van Ijzendoorn, and M. W. J. Prins, *ACS Nano*, 2012, **6**, 3134-3141.
 - 29 Y. K. Hahn and J. K. Park *Lab Chip* **2011**, *11*, 2045-2048.

- 1
2
3
4 30 M.A. Hayes, M.M. Petkus, A.A. Garcia, T. Taylor, P. Mahanti, *Analyst*, 2009, **134**, 533-
5 541.
6
7 31 Y. Zhang and D. Zhou, *Expert Reviews Ltd*, 2012, ISSN **1473-7159**, 565-571.
8
9 32 M.M. Petkus, M. McLauchlin, A.K. Vuppu, L. Rios, A.A. Garcia, M.A. Hayes,
10 *Analytical Chemistry*, 2006, **78**, 1405-1411.
11
12 33 Y.D. Zhu, J. Peng, L.P. Jiang, J.J. Zhu, *Analyst*, 2014, **139**, 649-655.
13
14 34 S. Sakamoto, K. Omagari, Y. Kita, Y. Mochizuki, Y. Maito, S. Kawata, S. Matsuda, O.
15 Itano, H. Jinno, H. Takeuchi, Y. Yamaguchi, Y. Kitagawa, H. Handa, *Clinical Chemistry*,
16 2014, **60**, 610-620.
17
18 35 C.F. Woolley, M.A. Hayes, *Bioanalysis*, 2013, **5**, 245-264.
19
20 36 Fluorescein-EX Protein Labeling Kit, 2004,
21 <http://tools.invitrogen.com/content/sfs/manuals/mp10240.pdf>.
22
23 37 L.A. Currie, *Analytical Chemistry*, 1968, **40**, 586-593.
24
25 38 Cardiac Marker ELISA Kits, 2013, [http://www.calbiotech.com/products/elisa-](http://www.calbiotech.com/products/elisa-kits/human-elisa-kits/cardiac-marker-elisa-kits)
26 [kits/human-elisa-kits/cardiac-marker-elisa-kits](http://www.calbiotech.com/products/elisa-kits/human-elisa-kits/cardiac-marker-elisa-kits).
27
28 39 Human Heart Fatty Acid Binding Protein ELISA Kit, 2015,
29 [http://www.mybiosource.com/prods/ELISA-Kit/Human/Heart-Fatty-Acid-Binding-](http://www.mybiosource.com/prods/ELISA-Kit/Human/Heart-Fatty-Acid-Binding-Protein/H-FABP/datasheet.php?products_id=20502)
30 [Protein/H-FABP/datasheet.php?products_id=20502](http://www.mybiosource.com/prods/ELISA-Kit/Human/Heart-Fatty-Acid-Binding-Protein/H-FABP/datasheet.php?products_id=20502).
31
32 40 Plasma Proteome Database, 2014, <http://www.plasmaproteomedatabase.org/index.html>.
33
34 41 P. Mahanti, T. Taylor, M.A. Hayes, D. Cochran, M.M. Petkus, *Analyst*, 2011, **136**, 365-
35 373.
36
37 42 E.G. Codding, *Analytical Chemistry*, 1979, **51**, 1981-1986.
38
39
40
41
42
43
44
45
46
47
48
49
50
51
52
53
54
55
56
57
58
59
60



A novel magnetic bead-based microimmunoassay achieves superior quantitation abilities for three cardiac biomarkers used in the diagnosis of myocardial infarction.

1
2
3
4
5
6
7
8
9
10
11
12
13
14
15
16
17
18
19
20
21
22
23
24
25
26
27
28
29
30
31
32
33
34
35
36
37
38
39
40
41
42
43
44
45
46
47
48
49
50
51
52
53
54
55
56
57
58
59
60